

**A Generalized K correction for Type Ia Supernovae:
Comparing R -band Photometry Beyond $z = 0.2$
with B , V , and R -band Nearby Photometry**

Alex Kim¹ and Ariel Goobar² and Saul Perlmutter³

Received _____; accepted _____

Submitted to *Publications of the Astronomical Society of the Pacific*

¹Center for Particle Astrophysics and Lawrence Berkeley Laboratory, 50-232, Berkeley, CA 94720; agkim@lbl.gov

²Physics Department, Stockholm University, Box 6730, S-113 85 Stockholm, Sweden; ariel@physto.se

³Lawrence Berkeley Laboratory, 50-232, and Center for Particle Astrophysics, University of California, Berkeley, CA 94720; saul@lbl.gov

ABSTRACT

Photometric measurements show that as a group nearby type Ia supernovae follow similar lightcurves and reach similar peak magnitudes (Branch & Tammann 1992). Thus, these supernovae can serve as standard candles or calibrated candles at cosmological distances. Magnitudes of local and distant supernovae, both in the same filter band, are compared using a K correction to account for the different spectral regions incident on that filter. A generalized approach compares magnitudes in different bands for the nearby and distant supernova, bands that are selected to give sensitivity in corresponding regions of the redshifted and unredshifted spectra. Thus at a redshift of $z \approx 0.5$, local B magnitudes are compared with distant R magnitudes. We compute these generalized K corrections over a range of redshifts and bandpass pairs and discuss their advantages over the traditional single-band K correction. In particular, errors near maximum light can be kept below 0.05 mag out to at least $z = 0.6$, whereas the traditional K correction is difficult to use beyond $z > 0.2$.

1. Introduction

Assuming no evolution and a homogeneous set of type Ia supernovae, a perfect and complete set of type Ia supernova spectra can be used to calculate the apparent magnitudes at any redshift and epoch, given the transmission functions and the zeropoints of the magnitude system. Unfortunately, this is not feasible due to several problems: (1) The available supernova spectra often have insufficient wavelength coverage to calculate broadband photometry and insufficient time coverage to track the quickly evolving supernova; (2) Many of the available spectra do not have the signal-to-noise to calculate precise magnitudes; (3) Spectral miscalibrations can lead to large errors in magnitude determinations; (4) The filter transmission function and detector response function are not perfectly known. More reliable magnitude calculations can be made using spectra and photometry together, photometry being less sensitive to the above problems than spectra. In this paper, we calculate and discuss the errors for a generalized K correction, an example of such a technique, with a preliminary analysis using three “normal” type Ia supernova. (One “peculiar” was also examined for comparison purposes.) These K corrections are particularly important for use with supernovae at $z > 0.2$, which are now being discovered in systematic searching (e.g., Perlmutter et al. 1994, 1995).

2. A Generalized K Correction

The standard K correction, K_x , is used to calculate the apparent magnitude in some “ x ” filter band of an object at redshift z according to the equation: $m_x(z, t) = M_x(t) + \mu(z) + K_x(z, t)$, where μ is the distance modulus (based on luminosity distance) and M_x is the absolute x magnitude (we omit explicit time dependence

in subsequent equations). The K correction relates nearby and distant magnitudes measured with the same filter:

$$K_x = 2.5 \log(1 + z) + 2.5 \log \left(\frac{\int F(\lambda) S_x(\lambda) d\lambda}{\int F(\lambda/(1+z)) S_x(\lambda) d\lambda} \right) \quad (1)$$

where $F(\lambda)$ is the spectral energy distribution at the source (in this case the supernova), and $S_x(\lambda)$ is the x 'th filter transmission (Oke & Sandage 1968).

We generalize this expression to handle different filters, adding a term that accounts for the differences in the zeropoints of the magnitude system:

$$\begin{aligned} K_{xy} &= -2.5 \log \left(\frac{\int \mathcal{Z}(\lambda) S_x(\lambda) d\lambda}{\int \mathcal{Z}(\lambda) S_y(\lambda) d\lambda} \right) + 2.5 \log(1 + z) + 2.5 \log \left(\frac{\int F(\lambda) S_x(\lambda) d\lambda}{\int F(\lambda/(1+z)) S_y(\lambda) d\lambda} \right) \\ &= -2.5 \log \left(\frac{\int \mathcal{Z}(\lambda) S_x(\lambda) d\lambda}{\int \mathcal{Z}(\lambda) S_y(\lambda) d\lambda} \right) + 2.5 \log \left(\frac{\int F(\lambda) S_x(\lambda) d\lambda}{\int F(\lambda') S_y(\lambda'(1+z)) d\lambda'} \right) \end{aligned} \quad (2)$$

where $\mathcal{Z}(\lambda)$ is an idealized stellar SED for which $U = B = V = R = I = 0$ in the photometric system being used. K_{xy} is thus defined so that $m_y = M_x + \mu + K_{xy}$. If $S_x \equiv S_y$, the first term drops out and this reduces to the standard K correction of Equation 1.

The second line of Equation 2 is a change of variables, $\lambda' = \lambda/(1+z)$, that makes it easier to understand the K_{xy} correction in the case $S_y(\lambda(1+z)) = S_x(\lambda)$, a situation approximated by the dashed lines in Figure 1. If the “blueshifted” y 'th filter matches the x 'th filter function the second term in this equation drops out, and one is left with the term accounting for the difference in zeropoints of the filters (this difference is the “color zeropoint”). In this case, spectral dependence on the correction is eliminated. Note that this cross-filter approach has previously been used for galaxy K corrections (e.g. Gunn 1978).

3. K_{xy} Calculation

We calculate generalized K corrections using Equation 2 with Bessell’s (1990) color zeropoints and realizations of the Johnson-Cousins UBVRI filter system (Figure 1). The color zeropoints are expected to match real photometric color zeropoints to better than 0.01 mag (Hamuy et al. 1992 quotes ≤ 0.009 , Bessell (private communication) quotes ≤ 0.005). Only supernovae with non-peculiar spectra and no evidence for reddening are used, as described by Vaughan et al. (1995). Our full sample is presented in Table 1 and contains 29 spectra from epochs $-14 < t_{max}^B < 76$ days after blue maximum for supernovae SN1981B, SN1990N, and SN1992A. The SN1981B data is from Branch et al. (1983), SN1990N data is described in Leibundgut et al. (1991), and SN1992A is in Suntzeff et al. (1995), and Kirshner et al. (1993). The SN1981B spectra labeled by epoch (0) is a composite of four spectra from March 6-9 (Branch et al. 1983). The SN1992A HST spectra from epoch 5 with a spectral range of 1650-4800 Å has been augmented by the CTIO spectra from epoch 6 as described in Kirshner et al. (1993); it is labeled epoch (5). The K corrections were not calculated for cases in which the spectra did not cover at least 99% of the effective acceptance of the passband and are labeled with ellipsis.

Tables 2, 3, and 4 have K_{xy} corrections for $x = B, V, R$, $y = R$ and redshifts spanning from 0 to 0.7 in increments of 0.025. Epochs are given in the supernova rest-frame. Note that K_{RR} is just the standard R band K correction. Each column of data is for a single supernova spectrum; the three tables have different number of columns because the number of spectra with sufficient wavelength coverage to calculate each correction varies. In particular, Table 4 has much fewer entries because there are only a few spectra covering the needed wavelength range to calculate K_{RR} . See Hamuy et al. for tables of K_{BB} and K_{VV} ; these K corrections have poor spectral coverage at $z > 0.1$ for K_{BB} and at $z > 0.3$ for K_{VV} .

4. Error Estimates and Determination of Optimal Filter Pair

We consider the contributions of the following sources of error in the K correction: numerical integration error, spectral measurement and calibration error, intrinsic supernova-to-supernova dispersion, instrumental effects, and zeropoint uncertainty.

The numerical integration is accurate to 0.001 mag and we are able to reproduce the standard K corrections in B and in V of Hamuy et al. to that accuracy. A larger source of uncertainty comes from the noise and calibration error of the spectra themselves. Lacking prior spectral error information, we test each spectrum’s error properties by calculating, for $z = 0$, $B - V$ colors on the subset of 24 spectra with sufficient coverage. Their difference from the photometrically observed colors form a Gaussian distribution with a sigma of 0.04 mag. These $B - V$ colors compare two spectral regions that have little overlap, while K corrections that compare overlapping regions are less sensitive to large scale miscalibrations and therefore should have smaller error.

The rapid but smooth evolution of supernova spectra should make K corrections a smooth function on the scale of a few days. However, the data shows scatter from measurement and calibration error in the spectra. The good temporal sampling of SN1992A allows us to make K correction error estimates based on this scatter. We illustrate by considering the specific examples of K_{BR} and K_{VR} at $z = 0.5$, shown in Figures 2 and 3. (Unfortunately, there are insufficient data points to similarly consider K_{RR} .) We first study the subset of SN1992A K corrections calculated from spectra measured at a single telescope, the CTIO 1.0-m. This includes all SN1992 spectra except the ones at epochs 5, 6, 9, 17, 46, and 76. We estimate the root-mean-square scatter of the data from a smooth curve to be < 0.002 for K_{BR} and < 0.02 for K_{VR} ; we take this to be the bound on the effects of spectral measurement errors. Considering the full sample of SN1992A K corrections from all the telescopes, we find the range (not the root-mean-square) in scatter to be ~ 0.004 for K_{BR} and ~ 0.1 for K_{VR} ; we take these to be the bounds on systematic instrumental error.

Having studied errors involved in the K corrections of a single type Ia supernova, we now consider the uncertainties involved in constructing a single K correction for this entire class of supernovae. We do this by examining systematic differences between the three supernovae in our sample. Again consider K corrections for $z = 0.5$ plotted in Figures 2 and 3. The scatter at a given epoch in K_{BR} and K_{VR} is dominated by intrinsic supernova-to-supernova differences. These differences are understood as being due to the observed variance in these particular supernovae’s color evolution, particularly around 20 days after maximum when the supernovae have quickly reached their reddest color. The range of scatter is ~ 0.015 mag for K_{BR} and ~ 0.2 mag for K_{VR} ; for epochs before day 17, the range narrows to < 0.002 for K_{BR} and ~ 0.1 mag for K_{VR} .

As a preliminary test of the variation in K correction for type Ia supernovae that are not “normal,” the K corrections of the “peculiar” type Ia SN1991T were also calculated (Ford et al. (1993) and Phillips et al. (1992) describe this supernova). Their scatter with respect to the normal supernovae’s K corrections was within the intrinsic supernova-to-supernova dispersion discussed above, even for epochs < 14 , when the SN1991T spectra least resembled “normal” type Ia spectra. This suggests that broadband averaging smooths over intrinsic differences in supernova spectra and that K corrections may be robust enough to use for the entire class of type Ia supernovae, although more examples of peculiar type Ia supernovae (e.g. SN1991bg) will be needed to test this possibility.

In the above discussions, no conclusions could be made on K_{RR} error due to sparseness of data. However, error estimates can be made based on the range of the correction. Recalling Equation 2, we see that K corrections are the sum of an overall offset due to the different filter zeropoints plus a spectrally dependent term. Smaller spectral terms will propagate smaller errors into the K correction than larger spectral terms. In this analysis, the relative size of the spectral term is apparent in the spread over time of the K correction,

since it is the only time-dependent term. Comparing the spread over time from Figure 4(a) with that from Figure 2, we see that the spectral contribution in the standard single-filter K correction, K_{RR} , is almost twice that of K_{VR} , showing that the errors in K_{RR} are much larger than those of K_{VR} . This point is demonstrated more dramatically in Figure 4(a,b) where K_{BR} and K_{RR} are plotted on the same scale. It is clear that the scatter in K_{BR} is much smaller than would be expected for K_{RR} .

We have examined potential instrumental effects by performing K_{xy} calculations with effective Kitt Peak 4-m passbands based on the quantum efficiency of the TK2B CCD camera and the KP1464 Harris B, KP1465 Harris V, and KP1466 Harris R filters for the B, V , and R filters respectively. Observations of standard stars show that this effective passband closely matches the Johnson-Cousins system, i.e. the color-correction term to transform from the instrumental to the photometric system is negligible. Comparison between these and the Bessell filter K corrections show differences at a level of 0.02 mag with standard deviation 0.02 mag. We also see the expected correlation with the observed supernova color; corrections for redder supernovae are more sensitive to the differences in the red tails of the Bessell and Kitt Peak response functions. (See Figure 5.) The nature of this dependence can be seen in Figure 6. A more detailed analysis will require a more complete spectral data set.

There is an additional error due to zeropoint uncertainty for K_{BR} and K_{VR} mag which does not effect K_{RR} . This is an advantage of the single-filter K correction, since zeropoints cancel if you compare data in the same band. As discussed earlier, the size of this error is less than 0.01 mag.

Given these contributing sources of error, we can compare the overall uncertainties for the generalized and standard K corrections. We begin with the case of $z = 0.5$. K_{BR} and K_{VR} have the same zeropoint uncertainty, however at this redshift K_{BR} has smaller

errors than K_{VR} from all other sources. This includes measurement error, instrumental systematics, and supernova-to-supernova systematics. Although K_{RR} has no zeropoint error, it is otherwise expected to have errors even larger than K_{VR} . We emphasize that K_{BR} has these advantages because at $z = 0.5$, $R(\lambda(1+z)) \approx B(\lambda)$, minimizing the spectral dependence on the K correction (Figure 1).

The case of $z = 0.5$ is important as an extreme in which it is possible to match filters. To illustrate the errors expected for other redshifts, Figure 7 also shows the calculated root-mean-square scatter for the group of K corrections near peak magnitude, for SN1992A at epochs -1 and 3, and SN1981B at epoch 0. The root-mean-square scatter is minimized at redshifts where the filters best match, and monotonically worsens as one moves away from these redshifts. Note that the error can be kept below 0.04 mag by switching from the nearby V photometry to the nearby B photometry when comparing supernovae at $z > 0.36$.

5. Conclusions

We have considered a generalized K correction as an alternative to the single-band K correction for relating local and high-redshift supernova magnitudes. Error sizes depend on the filter pair combination chosen and reflect the size of the term that accounts for the different spectral regions observed in distant and local supernovae. Minimizing this term by matching filters to observe the same region reduces error and can make a generalized K correction better than a single-band K correction. Matching filters also reduces the wavelength range needed to perform K corrections, making more of the available data usable for better temporal coverage and for studies in systematic differences in supernovae. Generally, error estimates and optimal filter pair determinations at any redshift can be made using a procedure similar to the one we have outlined for $z = 0.5$. Roughly, we find

that for $z < 0.1$, K_{RR} should be used, for $0.1 < z < 0.35$, K_{VR} should be used, and for $0.35 < z < 0.7$, K_{BR} should be used. Objects at higher redshift may be better observed in the I band.

These general results for the preferred observation bands at a given redshift to “match filters” will, of course, be true whatever the spectra observed. However, further studies based on more supernova spectra will improve the estimates of the generalized K corrections, and help characterize the detailed dependence on supernova-to-supernova variation.

We would like to thank B. Leibundgut, M. Bessell, D. Branch, and the Calan/Tololo Search Group (M. Phillips, N. Suntzeff, J. Maza, and M. Hamuy) for providing data and for helpful discussions. This work was supported in part by the National Science Foundation (ADT-88909616) and U. S. Department of Energy (DE-AC03-76SF000098).

REFERENCES

- Bessell, M. S. 1990, *PASP*, 102, 1181
- Branch, D., Falk, S. W., McCall, M. L., Rybski, P., Uomoto, A. K., and Wills, B. J. 1983, *ApJ*, 270, 123
- Branch, D., and Tammann, G. A. 1992, *ARA&A*, 30, 359
- Ford, C. H., Herbst, W., Richmond, M. W., Baker, M. L., Filippenko, A. V., Treffers, R. R., Paik, Y., and Benson, P. J. 1993, *AJ*, 106, 1101
- Gunn, J. E. 1978, in *Observational Cosmology : 8th advanced course of the Swiss Society of Astronomy and Astrophysics*, ed. A. Maeder, L. Martinet, and G. Tammann (Sauverny, Geneva)
- Hamuy, M., Phillips, M. M., Wells, L. A., and Maza, J. 1993, *AJ*, 105, 787
- Hamuy, M., Walker, A. R., Suntzeff, N. B., Gigoux, P., Heathcote, S. R., and Phillips, M. M. 1992, *PASP*, 104, 533
- Kirshner, R. P. et al. 1993, *ApJ*, 415, 589
- Kirshner, R. P., Blades, J. C., Branch, D., Chevalier, R. A., Fransson, C., Panagia, N., Wagoner, R. V., and Wheeler, J. C. 1988, *HST Proposal SINS: The Supernova Intensive Study*, unpublished
- Leibundgut, B. 1988, PhD thesis, University of Basel
- Leibundgut, B., Kirshner, R. P., Filippenko, A. V., Shields, J. C., Foltz, C. B., Phillips, M. M., and Sonneborn, G. 1991, *ApJ*, 371, L23
- Leibundgut, B., Tammann, G. A., Cadonau, R., and Cerrito, D. 1991, *A&AS*, 89, 537

Oke, J. B., and Sandage, A. 1968, ApJ, 154, 21

Perlmutter, S., Pennypacker, C. R., Goldhaber, G., Goobar, A., Muller, R. A.,
Newberg, H. J. M., Desai, J., Kim, A. G., Kim, M. Y., Small, I. A., Boyle, B. J.,
Crawford, C. S., McMahon, R. G., Bunclark, P. S., Carter, D., Irwin, M. J.,
Terlevich, R. J., Ellis, R. S., Glazebrook, K., Couch, W. J., Mould, J. R.,
Small, T., A., and Abraham, R. G. 1995. ApJ, 440, L41.

Perlmutter, S., et al. 1994. International Astronomical Union Circular, nos. 5956 and 5958.

Phillips, M. M., Wells, L. A., Suntzeff, N. B., Hamuy, M., Leibundgut, B., Kirshner, R. P.,
and Foltz, C. B. 1992, AJ, 103, 1632

Suntzeff, N. B. 1994, Private communication

Suntzeff, N. B. 1995, In preparation

Vaughan, T., Branch, D., Miller, D., and Perlmutter, S. In press. 1995, ApJ

TABLE 1
Selected Spectra of SNe Ia

SN	Epoch ^a	UT Date	Observatory/Tel	Observer(s)
1990N	-14	1990 Jun. 26.17	MMTO/MMT	Foltz
1990N	-7	1990 Jul. 02.99	CTIO/1.5-m	Phillips
1992A	-5	1992 Jan. 14.11	CTIO/1.0-m	Winge
1981B	-1(a)	1981 Mar. 6	McDonald/2.7-m	See Branch et al. (1983)
1981B	-1(b)	1981 Mar. 6	McDonald/2.7-m	See Branch et al. (1983)
1992A	-1	1992 Jan. 18.13	CTIO/1.0-m	Winge
1981B	(0) ^b	1981 Mar. 7	McDonald/2.7-m	See Branch et al. (1983)
1981B	0	1981 Mar. 7	McDonald/2.7-m	See Branch et al. (1983)
1992A	+3	1992 Jan. 22.04	CTIO/1.0-m	Winge
1992A	(+5) ^b	1992 Jan. 24	HST	SINSC ^c
1992A	+6	1992 Jan. 25.04	CTIO/1.5-m	Smith/Winkler
1992A	+7	1992 Jan. 26.04	CTIO/1.0-m	Winge
1990N	+7	1990 Jul. 17	Lick/3.0-m	Shields/Filippenko
1992A	+9	1992 Jan. 28.04	CTIO/1.5-m	Hamuy/Williams
1992A	+11	1992 Jan. 30.04	CTIO/1.0-m	Winge
1990N	+14	1990 Jul. 23.98	CTIO/4.0-m	Phillips/Baldwin
1992A	+16	1992 Feb. 04.04	CTIO/1.0-m	Winge
1981B	+17	1981 Mar. 24	McDonald/2.7-m	See Branch et al. (1983)
1992A	+17	1992 Feb. 05.04	CTIO/4.0-m	Hamuy
1990N	+17	1990 Jul. 27.16	MMTO/MMT	Huchra
1981B	+20	1981 Mar. 27	McDonald/2.7-m	See Branch et al. (1983)
1981B	+24	1981 Mar. 31	McDonald/2.7-m	See Branch et al. (1983)
1992A	+24	1992 Feb. 12.03	CTIO/1.0-m	Winge
1992A	+28	1992 Feb. 16.02	CTIO/1.0-m	Winge
1981B	+29	1981 Apr. 5	McDonald/2.7-m	See Branch et al. (1983)
1992A	+37	1992 Feb. 25.01	CTIO/1.0-m	Winge
1990N	+38	1990 Aug. 16.98	CTIO/1.5-m	Phillips
1992A	+46	1992 Mar. 05.02	CTIO/1.5-m	Phillips
1981B	+49	1981 Apr. 25	McDonald/2.1-m	See Branch et al. (1983)
1981B	+58	1981 May. 4	McDonald/2.7-m	See Branch et al. (1983)
1992A	+76	1992 Apr. 04.02	CTIO/4.0-m	Hamuy/Maza

^aEpoch relative to B maximum light.

^bSee text for discussion.

^cKirsher et al. (1988)

TABLE 2
 K_{BR} for SNe Ia

	$t_0^B = -14$	-7	-5	-1	(0)	3	(5)	6	7	9	11	14	16
z	SN 1990N	1990N	1992A	1992A	1981B	1992A	1992A	1992A	1992A	1992A	1992A	1990N	1992A
0.000	0.024	0.107
0.025	-0.042	0.013	...	-0.146	-0.228
0.050	-0.094	-0.043	...	-0.204	-0.285
0.075	-0.143	-0.128	-0.087	...	-0.263	-0.344	...	-0.387
0.100	-0.199	-0.180	-0.146	...	-0.326	-0.408	...	-0.470
0.125	-0.256	-0.223	-0.202	...	-0.371	-0.452	...	-0.515
0.150	-0.296	-0.248	-0.230	...	-0.396	-0.477	...	-0.544	-0.625	...	-1.142
0.175	-0.320	-0.271	-0.356	-0.365	-0.245	-0.418	-0.407	-0.488	-0.572	-0.560	-0.640	...	-1.135
0.200	-0.345	-0.303	-0.372	-0.379	-0.265	-0.435	-0.424	-0.503	-0.584	-0.577	-0.654	...	-1.117
0.225	-0.376	-0.342	-0.398	-0.408	-0.306	-0.467	-0.463	-0.538	-0.616	-0.618	-0.695	...	-1.118
0.250	-0.414	-0.388	-0.437	-0.452	-0.367	-0.512	-0.516	-0.584	-0.658	-0.665	-0.740	...	-1.116
0.275	-0.454	-0.427	-0.474	-0.490	-0.421	-0.545	-0.550	-0.609	-0.676	-0.682	-0.748	-0.795	-1.082
0.300	-0.488	-0.455	-0.499	-0.513	-0.453	-0.559	-0.562	-0.614	-0.675	-0.679	-0.741	-0.776	-1.039
0.325	-0.510	-0.474	-0.514	-0.525	-0.471	-0.567	-0.574	-0.619	-0.675	-0.680	-0.738	-0.763	-0.997
0.350	-0.532	-0.498	-0.540	-0.552	-0.502	-0.592	-0.603	-0.639	-0.686	-0.691	-0.740	-0.756	-0.955
0.375	-0.568	-0.539	-0.583	-0.594	-0.552	-0.628	-0.636	-0.665	-0.699	-0.702	-0.738	-0.750	-0.911
0.400	-0.615	-0.592	-0.629	-0.635	-0.606	-0.659	-0.663	-0.684	-0.707	-0.708	-0.733	-0.742	-0.867
0.425	-0.661	-0.644	-0.662	-0.666	-0.649	-0.682	-0.685	-0.699	-0.714	-0.715	-0.732	-0.743	-0.832
0.450	-0.696	-0.691	-0.695	-0.698	-0.691	-0.707	-0.709	-0.717	-0.726	-0.728	-0.739	-0.750	-0.803
0.475	-0.716	-0.717	-0.716	-0.714	-0.712	-0.714	-0.711	-0.716	-0.722	-0.725	-0.729	-0.737	-0.761
0.500	-0.715	-0.721	-0.709	-0.702	-0.701	-0.695	-0.689	-0.692	-0.694	-0.700	-0.698	-0.702	-0.704
0.525	-0.693	-0.706	-0.684	-0.679	-0.676	-0.668	-0.663	-0.663	-0.662	-0.670	-0.659	-0.665	-0.644
0.550	-0.654	-0.684	-0.657	-0.661	-0.659	-0.647	-0.640	-0.637	-0.632	-0.640	...	-0.631	...
0.575	-0.607	-0.678	-0.637	-0.650	-0.652	-0.631	-0.619	-0.611	-0.600	-0.607	...	-0.592	...
0.600	-0.562	-0.684	-0.647	...	-0.593	-0.580	...	-0.567	...	-0.549	...
0.625	-0.522	-0.689	-0.634	...	-0.560	-0.542	...	-0.519	...	-0.498	...
0.650	-0.480	-0.683	-0.608	...	-0.518	-0.494	...	-0.464	...	-0.441	...
0.675	-0.427	-0.663	-0.571	...	-0.469	-0.404	...	-0.379	...
0.700	-0.363	-0.631	-0.525	...	-0.416	-0.339	...	-0.310	...

TABLE 2
(Continued)

z	$t_0^B = 17$ SN 1981B	17 1990N	17 1992A	20 1981B	24 1981B	24 1992A	28 1992A	29 1981B	37 1992A	38 1990N	46 1992A	58 1981B	76 1992A
0.000	-0.558	-1.092	-1.817
0.025	-0.650	-1.157	-1.830
0.050	-0.776	-1.245	-1.847
0.075	-0.907	-1.319	-1.843	-1.504	-1.237
0.100	-0.985	-1.344	-1.806	-1.480	-1.238
0.125	-1.007	-1.165	-0.982	-1.328	-1.745	-1.438	-1.219	...	-0.804
0.150	-1.018	-1.161	-0.989	-1.308	-1.686	-1.426	-1.405	-1.405	-1.205	...	-0.820
0.175	-1.016	-1.149	-0.982	-1.278	-1.618	-1.394	-1.376	...	-1.351	-1.363	-1.177	...	-0.820
0.200	-1.007	-1.126	-0.965	-1.238	-1.542	-1.350	-1.337	...	-1.305	-1.313	-1.145	...	-0.837
0.225	-1.032	-1.123	-0.967	-1.224	-1.485	-1.316	-1.306	...	-1.272	-1.283	-1.137	...	-0.894
0.250	-1.063	-1.120	-0.969	-1.215	-1.431	-1.281	-1.269	...	-1.236	-1.253	-1.123	...	-0.925
0.275	-1.051	-1.085	-0.939	-1.172	-1.353	-1.226	-1.212	...	-1.183	-1.194	-1.081	...	-0.913
0.300	-1.016	-1.039	-0.900	-1.115	-1.266	-1.165	-1.153	-1.133	-1.126	-1.131	-1.032	...	-0.895
0.325	-0.980	-0.995	-0.867	-1.058	-1.184	-1.106	-1.095	-1.079	-1.072	-1.071	-0.987	...	-0.879
0.350	-0.945	-0.951	-0.838	-1.002	-1.104	-1.046	-1.036	-1.023	-1.014	-1.009	-0.940	...	-0.857
0.375	-0.905	-0.906	-0.811	-0.944	-1.027	-0.986	-0.976	-0.966	-0.956	-0.949	-0.891	...	-0.829
0.400	-0.861	-0.864	-0.788	-0.888	-0.955	-0.929	-0.920	-0.910	-0.903	-0.895	-0.852	...	-0.807
0.425	-0.823	-0.831	-0.777	-0.845	-0.897	-0.879	-0.874	-0.867	-0.860	-0.855	-0.827	...	-0.794
0.450	-0.797	-0.804	-0.775	-0.821	-0.854	-0.833	-0.831	-0.833	-0.820	-0.825	-0.803	...	-0.769
0.475	-0.760	-0.763	-0.758	-0.787	-0.801	-0.776	-0.775	-0.786	-0.765	-0.778	-0.757	...	-0.718
0.500	-0.704	-0.707	-0.723	-0.735	-0.734	-0.707	-0.710	-0.720	-0.698	-0.715	-0.699	...	-0.659
0.525	-0.644	-0.652	-0.690	-0.685	-0.669	-0.641	-0.649	...	-0.637	-0.659	-0.650	...	-0.607
0.550	...	-0.602	-0.660	-0.645	-0.615	-0.611	-0.604	-0.585	-0.550
0.575	...	-0.547	-0.625	-0.602	-0.558	-0.556	-0.550	-0.535	-0.484
0.600	...	-0.486	-0.587	-0.554	-0.498	-0.496	-0.491	-0.477	-0.411
0.625	...	-0.422	-0.543	...	-0.436	-0.424	-0.428	-0.410	-0.331
0.650	...	-0.354	-0.493	...	-0.368	-0.342	-0.363	-0.337	-0.246
0.675	...	-0.284	-0.439	-0.257	-0.297	-0.258	-0.155
0.700	...	-0.209	-0.380	-0.167	-0.227	-0.172	-0.055

TABLE 3
 K_{VR} for SNe Ia

z	$t_0^B = -14$	-7	-5	-1(a)	-1(b)	-1	(0)	0	3	(5)	6	7	7	9	11
	SN 1990N	1990N	1992A	1981B	1981B	1992A	1981B	1981B	1992A	1992A	1992A	1992A	1990N	1992A	1992A
0.000	0.008	0.038	-0.014
0.025	-0.058	-0.055	-0.047	-0.048	...	-0.091
0.050	-0.110	-0.111	-0.105	-0.106	...	-0.143
0.075	-0.159	-0.198	-0.156	-0.164	-0.164	...	-0.194	-0.114	...
0.100	-0.215	-0.249	-0.214	-0.227	-0.228	...	-0.251	-0.197	...
0.125	-0.272	-0.292	-0.270	-0.272	-0.272	...	-0.284	-0.243	...
0.150	-0.311	-0.317	-0.299	-0.297	-0.297	...	-0.297	-0.272	-0.271
0.175	-0.336	-0.341	-0.349	-0.331	-0.313	...	-0.319	-0.308	-0.308	-0.298	-0.300	-0.288	-0.285
0.200	-0.361	-0.373	-0.366	-0.345	-0.334	-0.323	-0.336	-0.326	-0.323	-0.310	-0.306	-0.305	-0.299
0.225	-0.392	-0.412	-0.392	-0.369	-0.371	-0.375	-0.374	-0.362	-0.369	-0.365	-0.358	-0.343	-0.333	-0.345	-0.340
0.250	-0.430	-0.458	-0.431	-0.426	-0.430	-0.418	-0.436	-0.421	-0.414	-0.417	-0.404	-0.384	-0.369	-0.393	-0.386
0.275	-0.470	-0.497	-0.468	-0.476	-0.481	-0.456	-0.490	-0.471	-0.447	-0.451	-0.430	-0.403	-0.388	-0.410	-0.394
0.300	-0.504	-0.525	-0.493	-0.504	-0.512	-0.479	-0.521	-0.499	-0.460	-0.464	-0.434	-0.402	-0.388	-0.407	-0.387
0.325	-0.526	-0.543	-0.507	-0.518	-0.529	-0.492	-0.539	-0.512	-0.468	-0.476	-0.439	-0.401	-0.388	-0.408	-0.384
0.350	-0.548	-0.567	-0.534	-0.540	-0.557	-0.518	-0.570	-0.540	-0.493	-0.504	-0.459	-0.413	-0.400	-0.419	-0.385
0.375	-0.584	-0.609	-0.577	-0.582	-0.607	-0.560	-0.621	-0.586	-0.529	-0.537	-0.485	-0.426	-0.421	-0.430	-0.384
0.400	-0.631	-0.662	-0.622	-0.629	-0.662	-0.602	-0.674	-0.636	-0.560	-0.565	-0.505	-0.434	-0.440	-0.435	-0.378
0.425	-0.677	-0.714	-0.656	-0.663	-0.705	-0.633	-0.718	-0.669	-0.583	-0.586	-0.519	-0.440	-0.454	-0.442	-0.378
0.450	-0.712	-0.760	-0.689	-0.664	-0.759	...	-0.608	-0.610	-0.537	-0.453	...	-0.456	-0.385
0.475	-0.732	-0.787	-0.709	-0.680	-0.781	...	-0.616	-0.612	-0.536	-0.448	...	-0.453	-0.375
0.500	-0.731	-0.791	-0.703	-0.668	-0.769	...	-0.596	-0.591	-0.512	-0.421	...	-0.428	-0.344
0.525	-0.709	-0.775	-0.678	-0.645	-0.745	...	-0.569	-0.564	-0.483	-0.388	...	-0.397	-0.304
0.550	-0.669	-0.754	-0.651	-0.628	-0.727	...	-0.548	-0.542	-0.457	-0.359	...	-0.368	...
0.575	-0.623	-0.747	-0.631	-0.616	-0.721	...	-0.532	-0.520	-0.431	-0.327	...	-0.334	...
0.600	-0.578	-0.754	-0.716	-0.495	-0.401	-0.294	...
0.625	-0.538	-0.759	-0.703	-0.461	-0.362	-0.247	...
0.650	-0.496	-0.753	-0.677	-0.419	-0.315	-0.192	...
0.675	-0.443	-0.732	-0.639	-0.371	-0.131	...
0.700	-0.379	-0.701	-0.594	-0.317	-0.066	...

TABLE 3
(Continued)

z	$t_0^B = 14$ SN 1990N	16 1992A	17 1981B	17 1992A	17 1990N	20 1981B	24 1981B	24 1992A	28 1992A	37 1992A	38 1990N	46 1992A	49 1981B	76 1992A
0.000	0.222	-0.072	-0.532
0.025	0.131	-0.137	-0.545
0.050	0.004	-0.226	-0.562
0.075	-0.127	-0.300	-0.558	-0.442	-0.348
0.100	-0.205	-0.324	-0.521	-0.418	-0.349
0.125	-0.227	-0.311	-0.283	-0.308	-0.460	-0.376	-0.330	...	-0.272
0.150	...	-0.303	-0.237	-0.307	-0.290	-0.288	-0.400	-0.342	-0.335	...	-0.343	-0.316	...	-0.289
0.175	...	-0.296	-0.236	-0.295	-0.282	-0.258	-0.333	-0.310	-0.306	-0.330	-0.301	-0.288	-0.275	-0.288
0.200	...	-0.278	-0.227	-0.273	-0.266	-0.219	-0.257	-0.267	-0.267	-0.283	-0.251	-0.256	-0.246	-0.305
0.225	...	-0.279	-0.252	-0.270	-0.268	-0.205	-0.199	-0.233	-0.236	-0.250	-0.221	-0.248	-0.249	-0.363
0.250	...	-0.277	-0.283	-0.266	-0.270	-0.196	-0.146	-0.197	-0.200	-0.215	-0.190	-0.234	-0.247	-0.393
0.275	-0.327	-0.243	-0.270	-0.231	-0.240	-0.153	-0.068	-0.142	-0.142	-0.162	-0.132	-0.192	-0.209	-0.382
0.300	-0.308	-0.200	-0.236	-0.185	-0.201	-0.095	0.019	-0.082	-0.083	-0.105	-0.069	-0.143	...	-0.364
0.325	-0.295	-0.158	-0.200	-0.141	-0.168	-0.038	0.102	-0.023	-0.025	-0.050	-0.009	-0.097	...	-0.347
0.350	-0.288	-0.116	-0.165	-0.097	-0.139	0.018	0.181	0.037	0.034	0.007	0.053	-0.050	...	-0.325
0.375	-0.281	-0.072	-0.125	-0.052	-0.112	0.075	0.258	0.098	0.094	0.065	0.113	-0.002	...	-0.298
0.400	-0.274	-0.029	-0.080	-0.010	-0.089	0.132	0.330	0.155	0.150	0.118	0.168	0.037	...	-0.275
0.425	-0.275	0.007	-0.043	0.023	-0.078	0.174	0.388	0.205	0.196	0.161	0.207	0.062	...	-0.262
0.450	-0.282	0.036	-0.017	0.050	-0.076	0.199	0.432	0.250	0.239	0.201	0.237	0.086	...	-0.237
0.475	-0.269	0.078	0.020	0.091	-0.059	0.232	0.484	0.308	0.295	0.256	0.284	0.133	...	-0.187
0.500	-0.234	0.135	0.076	0.147	-0.024	0.285	0.552	0.376	0.360	0.323	0.347	0.190	...	-0.128
0.525	-0.197	0.195	0.137	0.202	0.010	0.335	0.616	0.442	0.421	0.384	0.403	0.239	...	-0.075
0.550	-0.163	0.252	0.039	0.374	0.670	0.451	0.285	...	-0.018
0.575	-0.124	0.307	0.074	0.417	0.727	0.506	0.339	...	0.048
0.600	-0.081	0.368	0.112	0.466	0.787	0.566	0.398	...	0.121
0.625	-0.030	0.432	0.156	...	0.850	0.638	0.462	...	0.200
0.650	0.027	0.500	0.206	...	0.918	0.720	0.526	...	0.286
0.675	0.089	0.570	0.260	0.805	0.592	...	0.377
0.700	0.158	0.645	0.319	0.895	0.662	...	0.476

TABLE 4
 K_{RR} for SNe Ia

z	$t_0^B = -14$	0	(0)	7	17	20	24
	SN 1990N	1981B	1981B	1990N	1981B	1981B	1981B
0.000	0.000	0.000	0.000	0.000	0.000	0.000	0.000
0.025	-0.066	-0.084	-0.093	-0.078	-0.091	-0.065	-0.013
0.050	-0.118	...	-0.149	-0.129	-0.218	-0.153	-0.030
0.075	-0.167	...	-0.194	-0.180	-0.349	-0.227	-0.026
0.100	-0.223	...	-0.252	-0.237	-0.427	-0.252	0.011
0.125	-0.280	...	-0.308	-0.270	-0.449	-0.236	0.073
0.150	-0.319	...	-0.337	-0.283	-0.459	-0.216	0.132
0.175	-0.344	...	-0.352	-0.286	-0.458	-0.186	0.199
0.200	-0.369	...	-0.372	-0.292	-0.449	-0.146	0.275
0.225	-0.400	...	-0.412	-0.319	-0.474	-0.132	0.333
0.250	-0.438	...	-0.474	-0.356	-0.505	-0.123	0.386
0.275	-0.478	...	-0.528	-0.375	-0.492	-0.080	0.464
0.300	-0.512	...	-0.560	-0.375	-0.458	-0.023	0.551
0.325	-0.534	...	-0.578	-0.374	-0.422	0.034	0.634
0.350	-0.556	...	-0.608	-0.386	-0.387	0.090	0.713
0.375	-0.592	...	-0.659	-0.407	-0.347	0.148	0.790
0.400	-0.639	...	-0.712	-0.426	-0.302	0.204	0.862
0.425	-0.685	...	-0.756	-0.440	-0.265	0.247	0.920
0.450	-0.720	...	-0.798	...	-0.239	0.271	0.964
0.475	-0.740	...	-0.819	...	-0.202	0.305	1.016
0.500	-0.739	...	-0.807	...	-0.146	0.357	1.084
0.525	-0.717	...	-0.783	...	-0.085	0.407	1.148
0.550	-0.677	...	-0.765	0.447	1.202
0.575	-0.631	...	-0.759	0.489	1.259
0.600	-0.586	...	-0.754	0.538	1.319
0.625	-0.546	...	-0.741	1.382
0.650	-0.504	...	-0.715	1.450
0.675	-0.451	...	-0.677
0.700	-0.387	...	-0.632

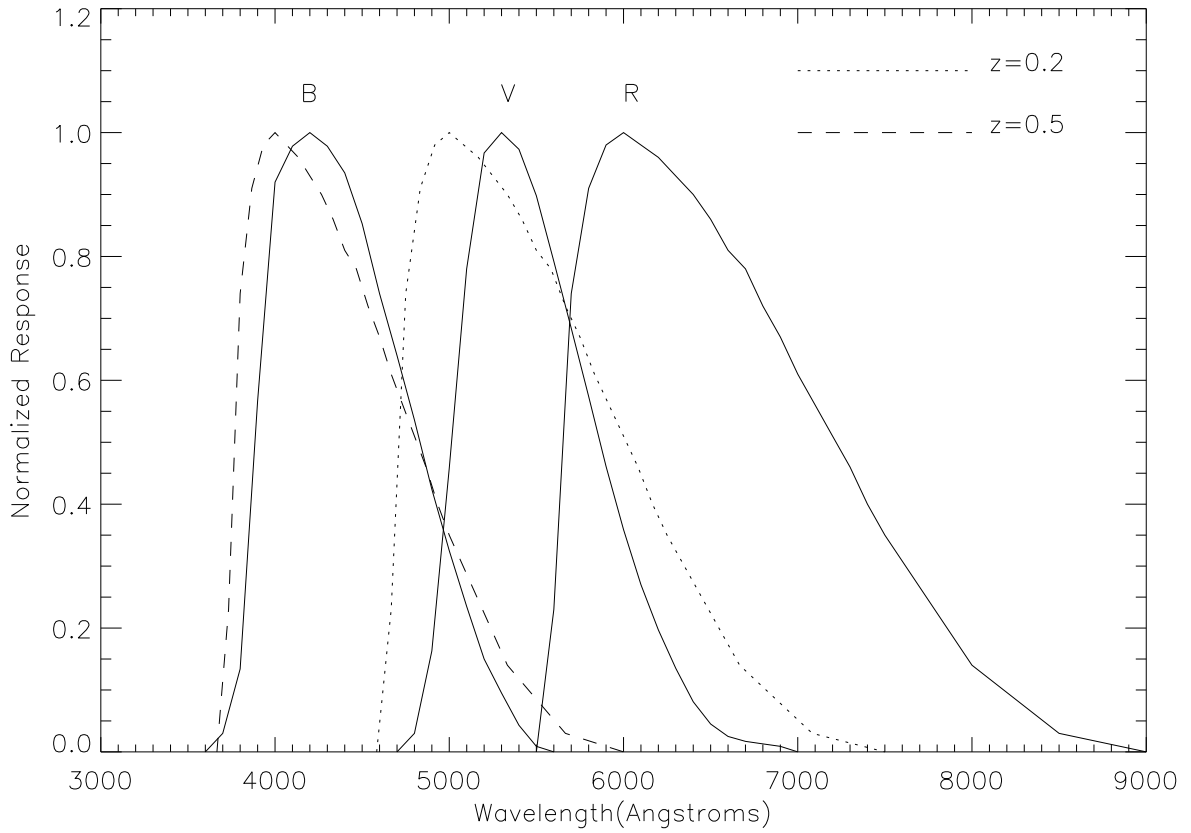


Fig. 1.— Bessell’s representations of the Johnson-Cousins B , V , and R passbands. The dotted lines represent the blue-shifted R filter for $z = 0.2$ and $z = 0.5$. The R filter approximately matches the V and B filters at these redshifts.

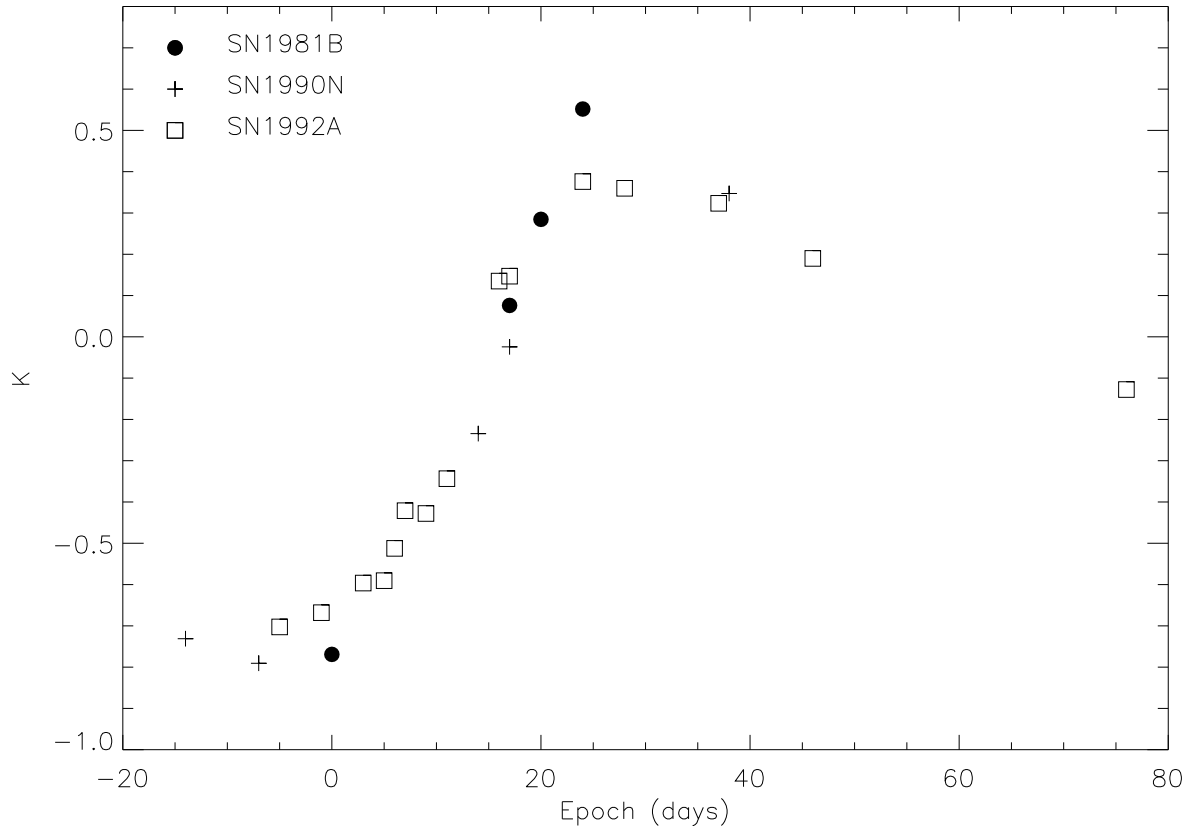


Fig. 2.— $K_{VR}(z = 0.5)$ as a function of epoch for SN1981B, SN1990N, and SN1992A.

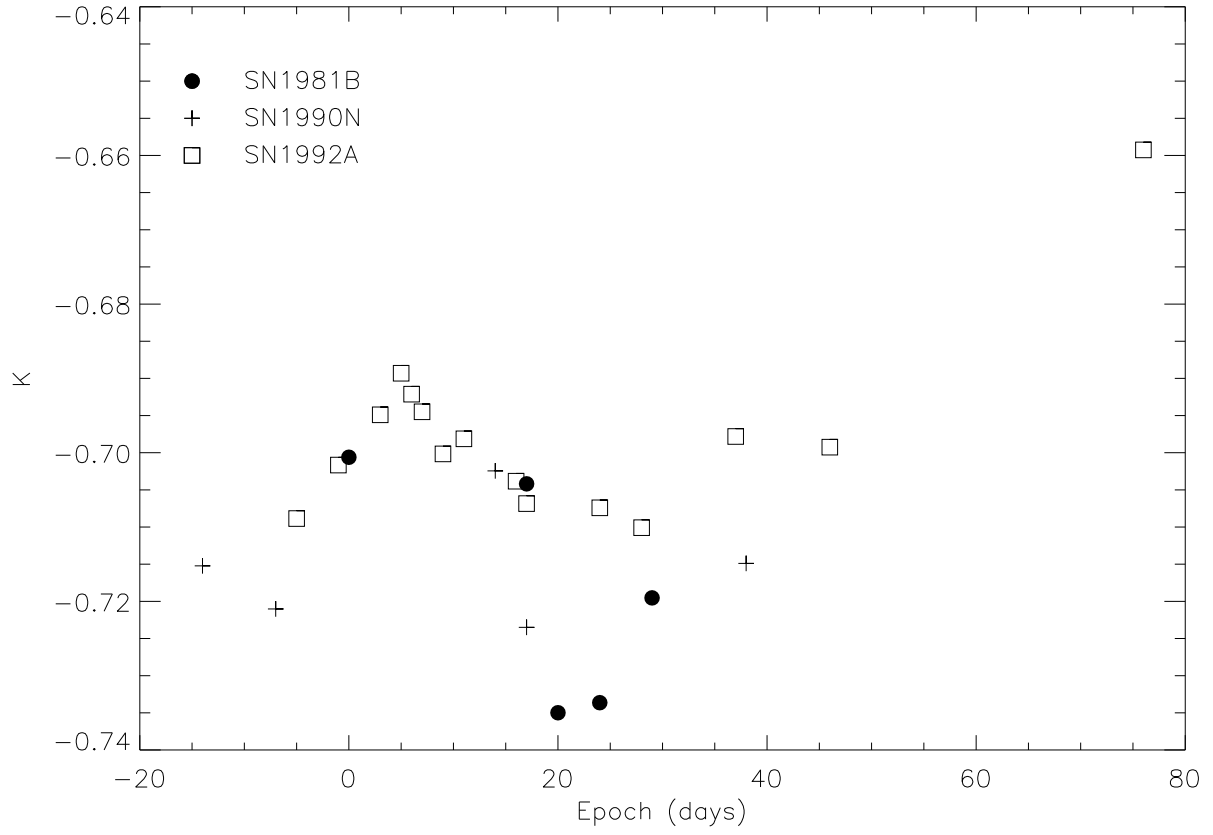


Fig. 3.— $K_{BR}(z = 0.5)$ as a function of epoch for SN1981B, SN1990N, and SN1992A. The same data as in Figure 5(b) but on a blown up scale.

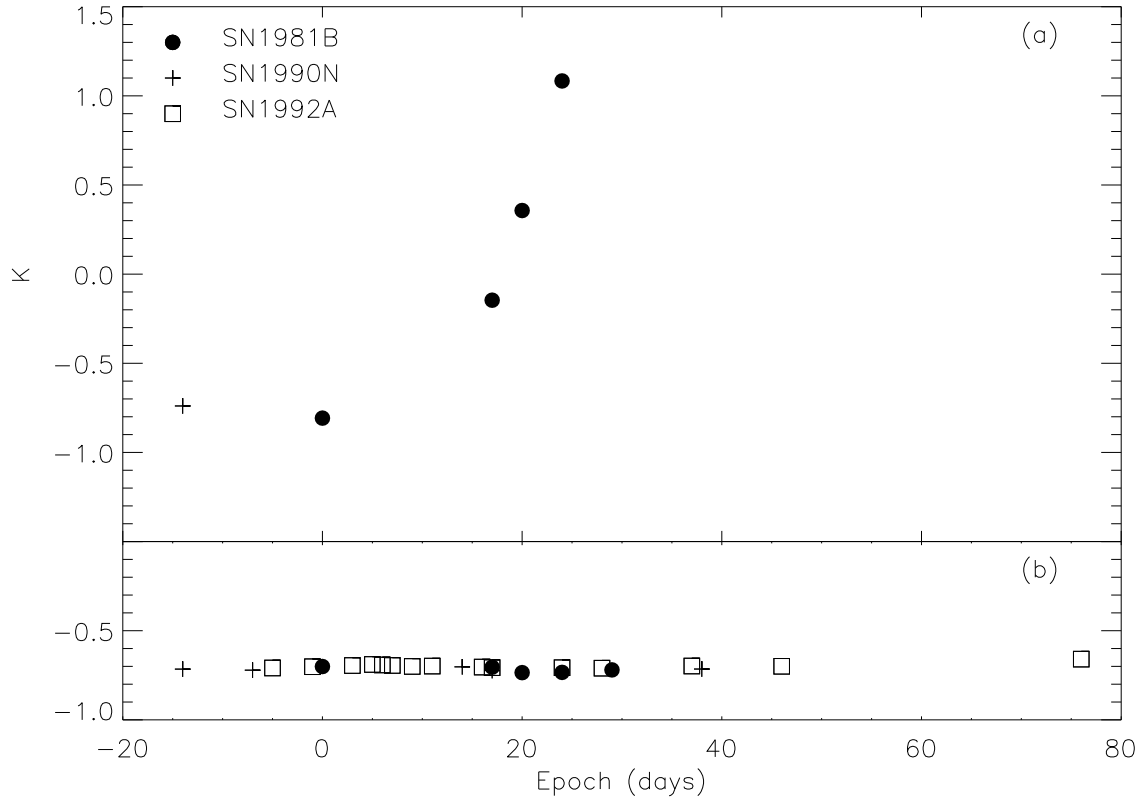


Fig. 4.— (a) $K_{RR}(z = 0.5)$ (or the R band K correction) as a function of epoch for SN1981B and SN1990N. The available spectra of SN1992A does not have sufficient coverage to make such a calculation. (b) $K_{BR}(z = 0.5)$ plotted on the same scale as (a) to show the relative ranges of the two corrections.

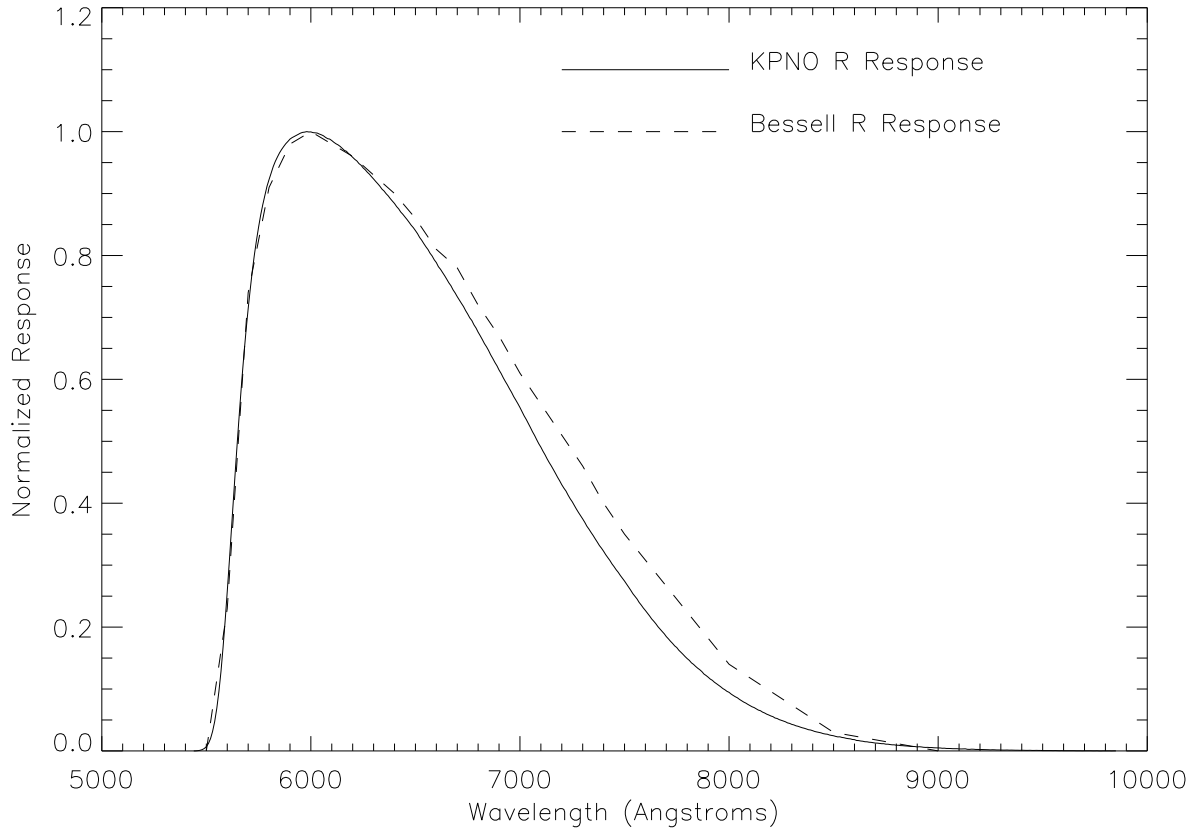


Fig. 5.— Comparison between the Bessell representation of R and our constructed response of the KPNO R as described in the text, normalized at peak transmission.

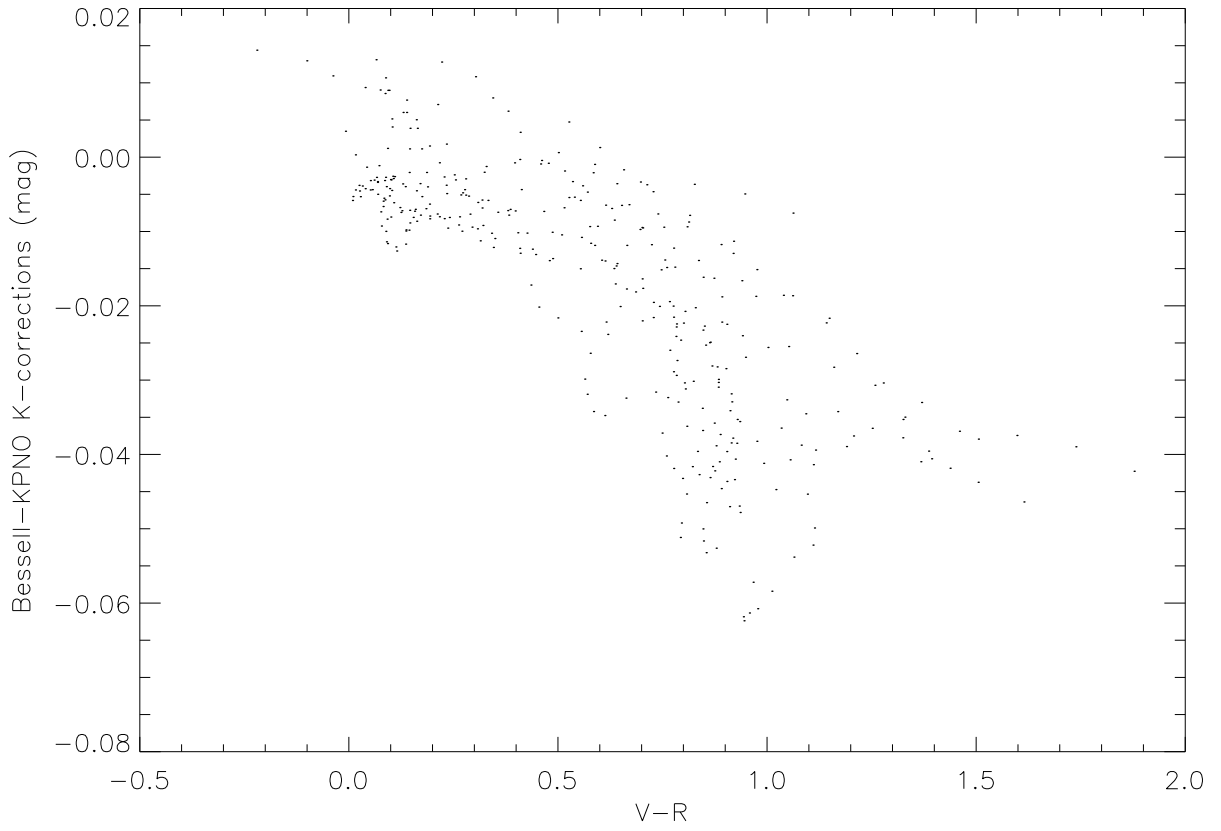


Fig. 6.— $K_{BR}(Bessell) - K_{BR}(KPNO)$ as a function of observed color for all redshifts.

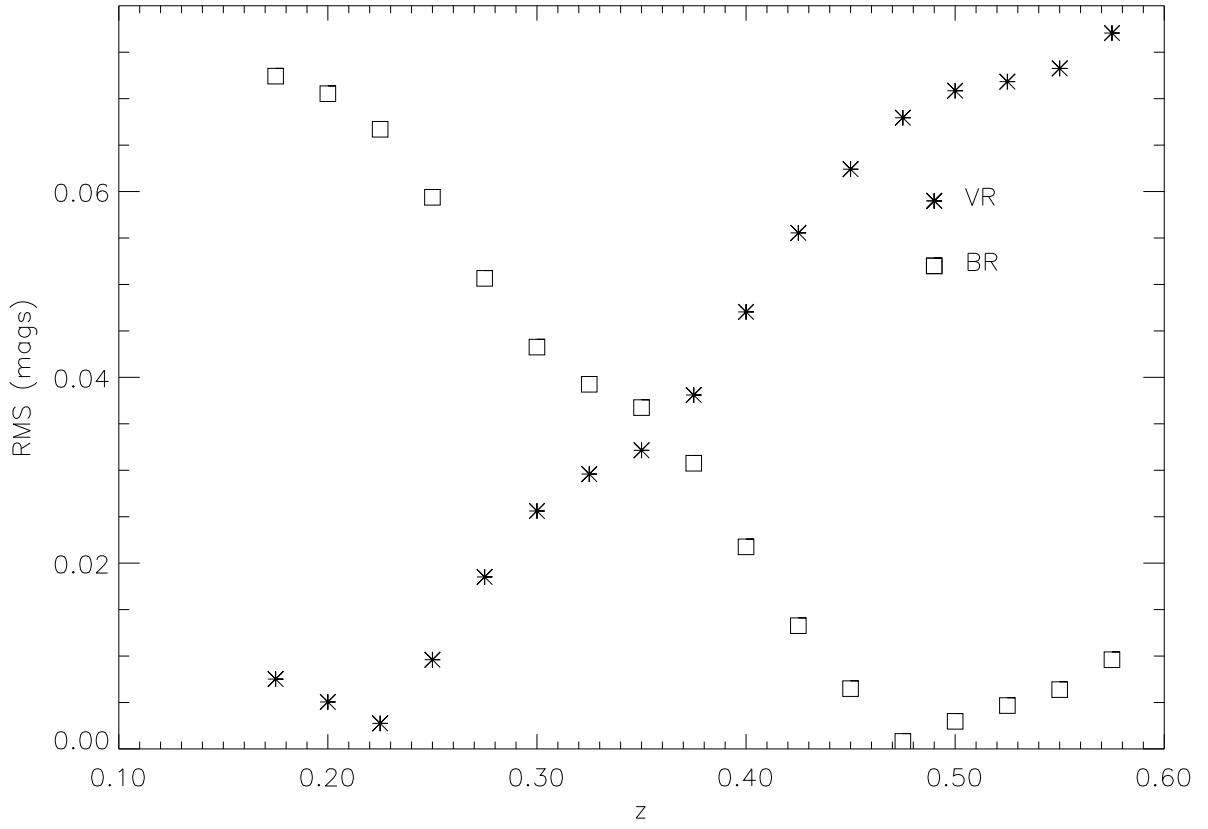


Fig. 7.— The root-mean-square scatter of K_{BR} (squares) and K_{VR} (stars) for SN1992A at epochs -1 and 3, and SN1981B at epoch 0 as a function of redshift.